

## Shrinkage of highly oriented gel-spun polymeric fibres

D. J. Dijkstra and A. J. Pennings\*

Department of Polymer Chemistry, University of Groningen, Nijenborgh 16,  
NL-9747 AG Groningen, The Netherlands

### Summary

The melting and shrinking process of gel-spun hot-drawn UHMWPE fibres has been investigated. Instead of being superheated, the highly oriented fibres start to melt at the fibre ends and shear bands, at a temperature near the equilibrium melting temperature of polyethylene. For draw ratios of  $\lambda \geq 40$ , the fibre transforms into a ribbon shape upon melting. This change in shape could be prevented by constrained heating before shrinkage. 'Ribbon-like melting' was also observed for gel-spun hot-drawn poly(L-lactide) fibres.

### Introduction

Polymers with ultra-high modulus and strength can be produced by a variety of routes, e.g. hot-drawing of gels (1-3), oriented crystallization of entanglement networks (4-6), hydrostatic extrusion of semi-crystalline polymers in combination with hot-drawing (7-9). In all these routes, the efficiency of inducing and maintaining chain extension is crucial in producing high modulus and strength products (10).

Prevorsek and Tobolsky (11) described a method giving information about the chain extension and orientation. They determined the non-flow shrinkage ratio of oriented fibres, and showed the dimensional changes accompanying the transition of an oriented semi-crystalline molecular structure into a disoriented amorphous random coil structure for various types of fibres. Shrinkage measurements on oriented materials were already carried out by several workers (12-15) and has now become a standard technique for the determination of the deformation efficiency (10,16).

To acquire information about the molecular conformation, and to gain a better understanding of the hot-drawing process, we have undertaken an investigation of the melting and shrinkage behaviour of ultra-high molecular weight polyethylene (UHMWPE) fibres, which were hot-drawn to various draw ratios.

Shrinkage measurements on gel-spun UHMWPE fibres hot-drawn to a ratio of  $\lambda \geq 40$ , showed a remarkable change in macroscopic shape. These fibres were transformed into ribbons upon melting, starting at the fibre ends or at shear bands. Differential scanning calorimetry (DSC) measurements on chopped fibres at low scanning rates, revealed a curve with many separate melting peaks.

The transformation of UHMWPE fibres into the ribbon-shaped material could be prevented, if the shrinkage measurements were performed on fibres that were first heated to a temperature of 150 °C with both fibre ends fixed, before the fibre was allowed to shrink. Fibres, with a draw ratio of  $\lambda \geq 40$  shrunk in this way, revealed a shrinkage ratio of about  $\lambda_s = 8$ , from which was concluded that the shrinkage was due to the melting of the crystalline blocks in the fibre.

'Ribbon-shaped melting' was also observed for and poly(L-lactide) gel-spun hot-drawn fibres.

\* To whom offprint requests should be sent

## Experimental

Ultra-high strength polyethylene fibres used in this study were obtained by hot drawing of porous polyethylene obtained by gel-spinning of UHMWPE ( Hifax 1900, by Hercules :  $M_w = 4 \cdot 10^6$  kg/kmol,  $M_n = 5 \cdot 10^5$  kg/kmol ), as described previously (17).

Samples with the following draw ratios were used :  $\lambda = 0, 10, 20, 30, 40, 50, 60, 80$  and  $100$ .

Differential scanning calorimetry ( DSC ) measurements were performed using a Perkin Elmer DSC-7. Indium standards were used for temperature calibrations. Various scanning rates were used from  $0.1$  to  $5$  °C/min. For the very low scanning rate of  $0.1$  °C/min, the extended data mode was used.

To examine the melting behaviour of the drawn monofilaments, two methods of sample preparation were adopted. Unconstrained melting was performed on filaments which had been cut into small pieces of about 3 mm in length. These were placed in aluminium sample pans together with a droplet of silicone oil, to provide good thermal contact between sample and pan (18). Constrained melting of the filaments was conducted by winding a piece of fibre, ca. 30 cm in length, tightly around an aluminium frame . The fibre ends were knotted and loose ends were cut off. In this way the length of the fibre was kept constant during heating. These constrained samples were placed in aluminium sample pans together with a droplet of silicone oil.

The shrinkage measurements were performed with and without constrained pre-heating. For shrinkage experiments without constrained pre-heating, the sample was placed into a glass container filled with silicone oil. This glass container was subsequently placed into a thermostated silicone oil bath of the desired temperature. The shrinkage of the fibre could be visually followed through a glass window in the oil bath. For the shrinkage measurements with constrained pre-heating, ca. 50 cm of fibre was clamped between two stainless steel clamps. The fibre was placed into the silicone oil bath at fixed fibre length. The clamped fibre was marked at several places with ink traces in order to be able to calculate the shrinkage ratio from the decrease in length between them. After the fibre had reached the desired temperature, the distance between the clamps was reduced in order to allow the fibre to shrink, until the shrunk fibre was lax.

Wide-angle X-ray scattering ( WAXS ) patterns were obtained using a Statton camera (19), equipped with pinhole optics, a vacuum path and flat photographic plates.

The poly( L- lactide ) fibres were gel-spun hot-drawn mono-filaments kindly supplied by Drs. A. R. Postema, Laboratory of Polymerchemistry, University of Groningen, the Netherlands.

## Results and Discussion

Upon constrained melting, shrinkage of the filaments is prevented. Under such circumstances the recoiling of the molecules is strongly hampered by the physical entanglements in the disordered domains (20), leading to superheating. The superheating of flexible, linear macromolecules was first studied by Wunderlich (21). Detailed experiments on superheating by Hellmuth and Wunderlich (22) on various crystals of polyethylene revealed considerable peak temperature elevations on differential thermal analysis.

For chain-extended polyethylene the orthorhombic structure is no longer stable above  $150$  °C and transforms into the hexagonal or rotator phase (20). In the hexagonal phase the chains can easily slip past one another and the transient network will disentangle. The disentanglement leads to fibre breakage and recoiling.

Figure 1 shows the constrained melting DSC thermogram of a gel-spun UHMWPE fibre hot-drawn to a ratio of  $\lambda = 100$ . The phase-transition peak-temperature is recorded at  $152$  °C. the second peak is ascribed to the melting of the hexagonal phase and the heat take-up resulting from the trans-gauge conformational changes (20) . In figure 1 also the unconstrained, i.e. chopped fibre, DSC thermogram ( scanspeed :  $5$  °C/min ) is shown of a fibre identical the one described above. A melting point with several peaks is recorded at about  $142$  °C, a temperature near the equilibrium melting point of polyethylene (23).

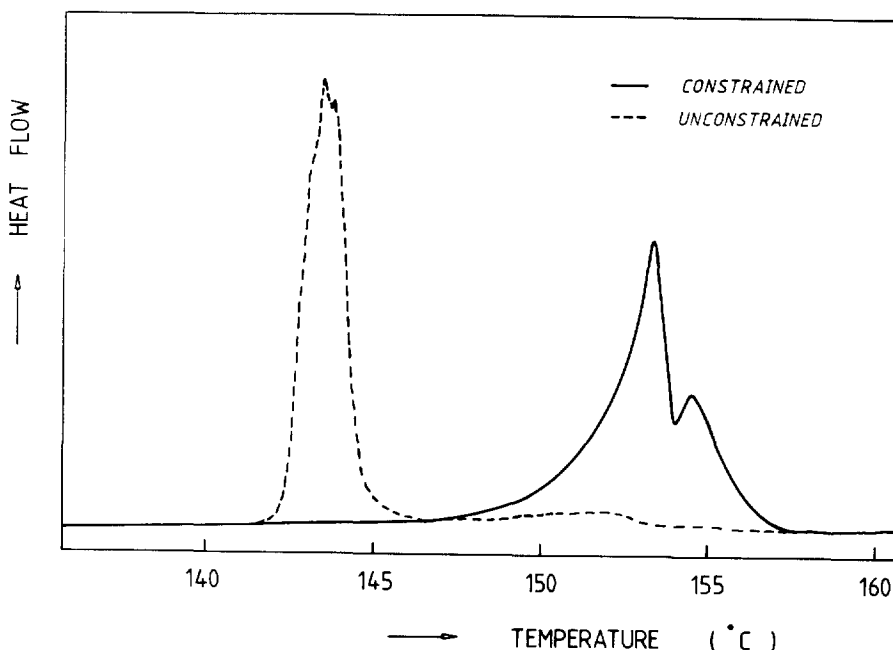


Figure 1 : Melting thermograms, recorded at a scanspeed of  $5^{\circ}\text{C}/\text{min}$  in DSC, of gel-spun hot-drawn UHMWPE fibres.

In figure 2 the unconstrained melting thermogram is recorded at a scanspeed of  $0.1^{\circ}\text{C}/\text{min}$  instead of  $5^{\circ}\text{C}/\text{min}$ . Between  $142$  and  $143^{\circ}\text{C}$  a spectrum of very small melting peaks is recorded for the chopped UHMWPE fibre. Every piece of chopped fibre seems to melt independently from the rest of the sample. DSC-thermograms of UHMWPE powder and constrained UHMWPE fibre both at this low scanspeed, taken to preclude the possibility of artefacts, revealed only one single melting peak.

The melting peak for unconstrained melting in figure 1 is, due to the high scanspeed, probably the envelope of the melting peaks shown in figure 2.

Unconstrained melting experiments were also performed in a large thermostated silicone oil bath, in order to follow the melting process visually. A glass container, containing the fibre in silicone oil at room temperature, was submerged in the thermostated oil bath. The temperature in the glass container is now slowly increasing towards the temperature of the oil bath. At a temperature of about  $142^{\circ}\text{C}$  the ends of the fibre ( $\lambda \geq 40$ ) suddenly change from a fibre with a cylindrical shape into one with a ribbon shape (see figure 3). 'Ribbon-shaped melting' also started at places where shear-bands were introduced by sharply bending the fibre. The ribbon grows very slowly in a direction perpendicular to the rest of the fibre, and seems to swallow it up gradually.

'Ribbon-shaped melting' is observed only for UHMWPE fibres with a draw ratio of  $\lambda \geq 40$ . For draw ratios  $\lambda < 40$ , normal cylindrical shrinkage is observed. This cylindrical shrinkage takes place in a fraction of a second, whereas 'ribbon-shaped melting' for the fibres with high draw ratio is substantially slower.

The initial hot-drawn fibre is highly fibrillar. Figure 4 shows how these fibrils are transformed into layers in the ribbon. Wide-angle X-ray scattering (WAXS) experiments on ribbon-shaped samples, cooled down to room temperature, revealed that the ribbons are highly oriented. Figure 5 shows the WAXS diffraction pattern. The chain axis seems to be preferentially aligned perpendicular to both fibre axis and ribbon-growth direction.

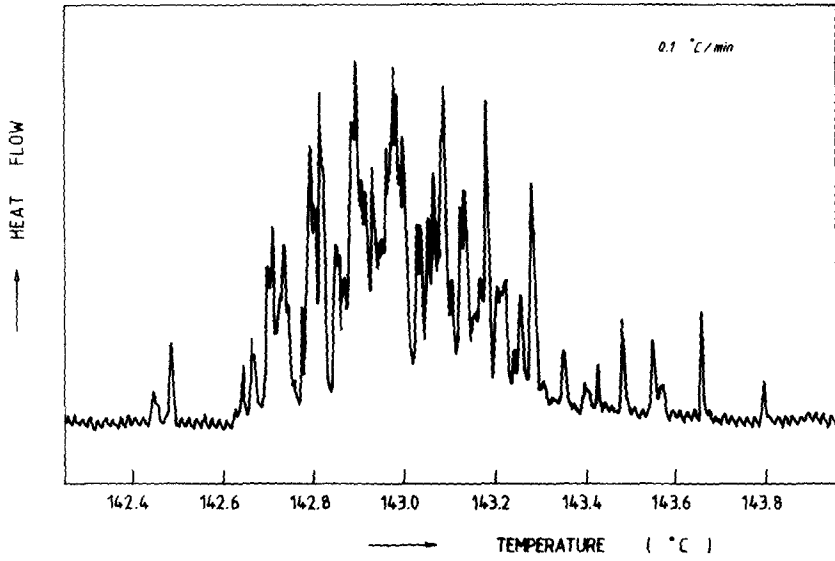


Figure 2 : Melting thermogram of unconstrained, chopped gel-spun hot-drawn UHMWPE fibre, recorded at a scanspeed of 0.1 °C/min.

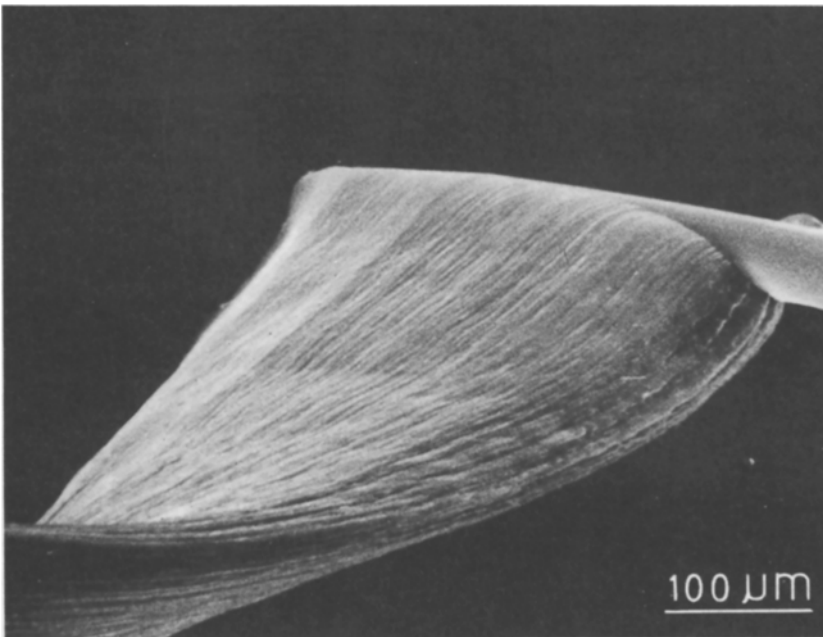


Figure 3 : SEM micrograph of a ribbon, formed upon melting of a UHMWPE fibre.

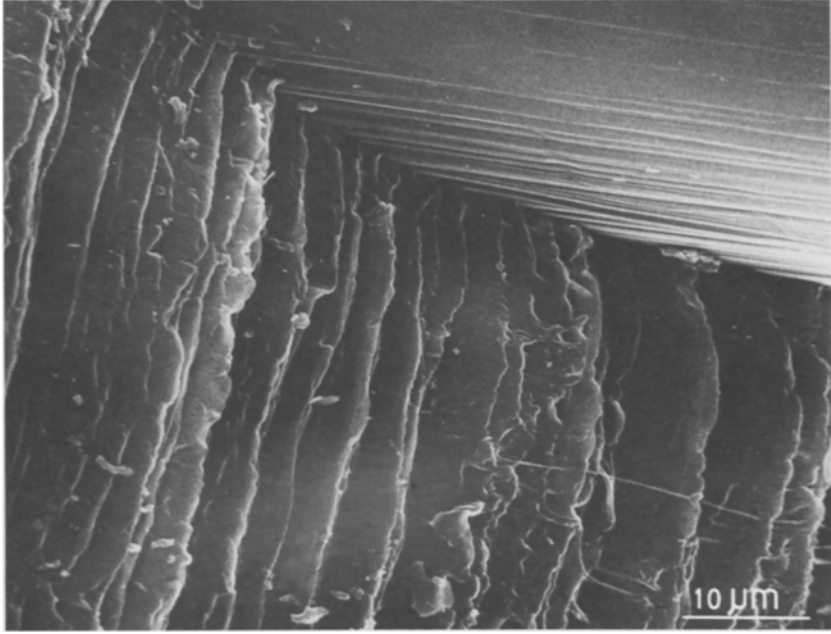


Figure 4 : SEM micrograph of the melting front of figure 3. The layered structure of the ribbon can be seen at the bottom of the micrograph.

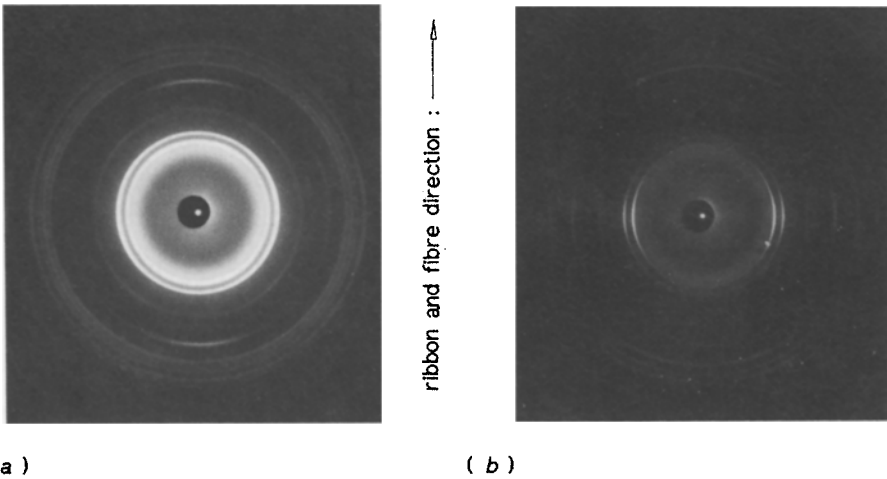


Figure 5 : WAXS patterns of a : ( a ) crystallized ribbon, formed upon melting of a gel-spun hot-drawn UHMWPE fibre, ( b ) constrained-preheated shrunk, recrystallized gel-spun hot-drawn UHMWPE fibre

'Ribbon-shaped melting' was also observed for another type of highly oriented gel-spun hot-drawn polymeric fibre. Figure 6 shows the 'ribbon-like melting' of a poly ( L- lactide ) ( PLLA ) fibre.

'Ribbon-like' shrinkage can be avoided by means of constrained heating , i.e. the fibre is heated to 150°C with both fibre ends fixed, before the fibre is allowed to shrink. Fibres shrunk this way remained cylindrical in shape for all draw ratios.

Fibres with a draw ratio of  $\lambda = 100$  that were constrained heated to 145 ° C shrunk ribbon-shaped, indicating that the shape transition depends critically on the constrained heating temperature. The quotient of fibre length before and after constrained heating and shrinkage, is shown in figure 7 as a function of the draw ratio. After an initial increase at low draw ratios, a plateau in the shrinkage is reached at a draw ratio of about  $\lambda = 40$ .

The theoretical shrinkage of a fibre with length  $L$ , corresponds to the complete randomization of fully extended molecules, which are randomly packed in the crystal lattice, and is given by the equation :

$$\lambda_s = \frac{L \text{ ( before shrinkage )}}{L \text{ ( after shrinkage )}} = \frac{l_0}{2 R_g} \quad ( 1 )$$

where  $l_0$  represents the contour length and  $R_g$  the radius of gyration in the fully relaxed melt. For polyethylene the quantities  $l_0$  and  $R_g$  can be related to each other by the formula ( 3 ) :

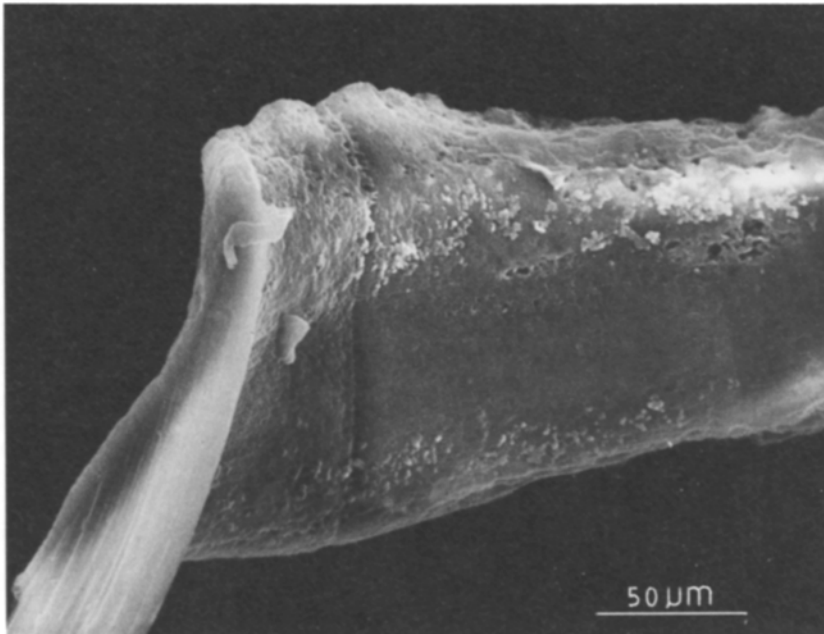


Figure 6 : SEM micrograph of the melting front of a gel-spun hot-drawn PLLA fibre

$$\frac{l_0}{2 R_g} = 0.39 \cdot \sqrt{n} \quad (2)$$

where  $n$  is the number of chain units. For a shrinkage ratio of 8, a contour length of about  $l_0 = 50$  nm can be calculated from equation 2, a length close to the crystal-block length of 70 nm observed in dark-field electron-microscopy and wide-angle X-ray scattering measurements (24). The WAXS pattern in figure 5b shows that still some orientation is left after shrinkage of constrained heated fibres. This might explain the small difference in contour length between the calculations from constrained-heated shrinkage and dark-field electron-microscopic measurements.

The entanglements in the disordered domains, located between the crystal blocks (25), hinder the chains upon shrinkage. This seems to have quite a bit in common with the observations by Mandelkern et.al. (14), who showed that crosslinking of oriented polyethylene results in a decrease in shrinkage ratio.

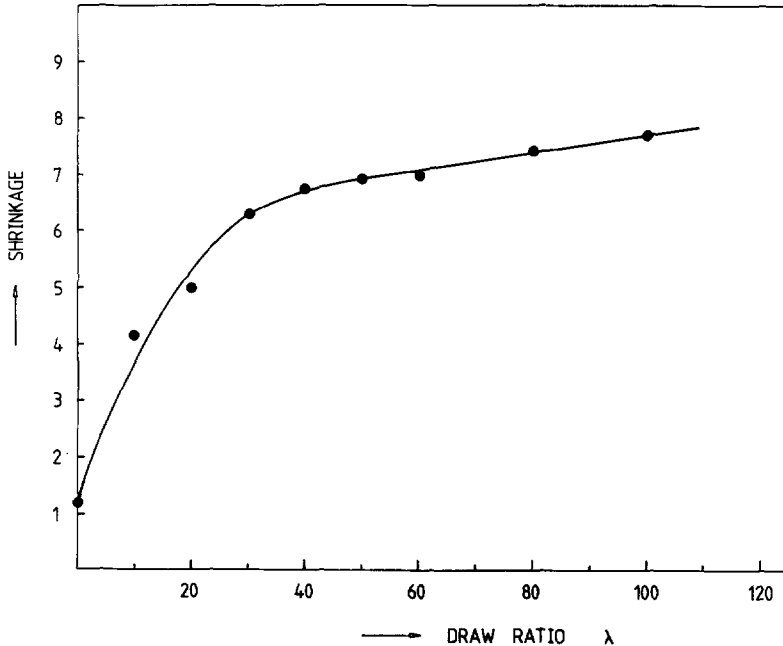


Figure 7 : The shrinkage, quotient of the sample length before and after (constrained preheated) shrinkage, as a function of the hot-draw ratio of a gel-spun UHMWPE fibre

### Conclusions

No superheating was observed upon melting of gel-spun hot-drawn UHMWPE fibres. Instead of being superheated, the fibres start to melt at the fibre ends and shear bands, at a temperature near the equilibrium melting temperature of polyethylene. For draw ratios of  $\lambda \geq 40$ , superheating seems to be avoided by a change in macroscopic shape, the fibre transforms into a ribbon shape upon melting. 'Ribbon-like melting' is also observed for PLLA gel-spun hot-drawn fibres.

Constrained-heated shrinkage experiments, i.e. heating the fibre with fibre ends fixed in space to a temperature above the melting temperature before shrinkage is allowed, showed that:

- the crystal blocks, between disordered domains with entanglements, shrink separately. The shrinkage ratio of the fibre is determined by the contour length of the chain in the crystal block.
- the conformation of the chains in the gel-spun fibre does not seem to change much beyond hot-draw ratios of  $\lambda = 40$ .

#### Acknowledgement

This study was supported by the Netherlands Foundation for Chemical Research ( S.O.N. ) with financial aid from the Netherlands Organization for the Advancement of Pure Research ( Z.W.O. ).

#### References

1. B. Kalb, A. J. Pennings, *Polym. Bull.* 1, 871 ( 1979 )
2. B. Kalb, A. J. Pennings, *Polymer* 21, 3 ( 1980 )
3. B. Kalb, A. J. Pennings, *J. Mater. Sci.* 15, 2584 ( 1980 )
4. A. J. Pennings, A. Zwijnenburg, *J. Polym. Sci., Polym. Phys. Ed.* 17, 1011 ( 1979 )
5. D. T. Grubb, M. J. Hill, *J. Cryst. Growth* 48, 321 ( 1980 )
6. G. Capaccio, I. M. Ward, *Coll. Polym. Sci.* 260,46 ( 1982 )
7. G. Capaccio, A. G. Gibson, I. M. Ward, 'Ultra-High Modulus Polymers', A. Cifferri and I. M. Ward Eds., Applied Science Publishers, London, 1 ( 1979 )
8. A. E. Zachariades, W. T. Mead, R. S. Porter, *Chem. Rev.* 85, 351 ( 1980 )
9. A. E. Zachariades, W. T. Mead, R. S. Porter, 'Ultra-High Modulus Polymers', A. Cifferri and I. M. Ward Eds., Applied Science Publishers, London, 77 ( 1979 )
10. M. P. C. Watts, A. E. Zachariades, R. S. Porter, *J. Mater. Sci.* 15, 426 ( 1980 )
11. D. Prevorsek, A. V. Tobolsky, *Textile Research J.* 33, 795 ( 1963 )
12. P. J. Flory, *J. Am. Chem. Soc.* 78, 5222 ( 1956 )
13. J. F. M. Oth, P. J. Flory, *J. Am. Chem. Soc.* 80, 1297 ( 1958 )
14. L. Mandelkern, D. E. Roberts, A. F. Diorio, A. S. Posner, *J. Am. Chem. Soc.* 81, 4148 ( 1959 )
15. D. E. Roberts, L. Mandelkern, *J. Am. Chem. Soc.* 80, 1289 ( 1958 )
16. G. Lopatin, *J. Appl. Polym. Sci. : Appl. Polym. Symp.* 31,127 ( 1977 )
17. J. Smook, M. Flinterman, A. J. Pennings, *Polym. Bull.* 5, 317 ( 1981 )
18. N. E. Weeks, R. S. Porter, *J. Polym. Sci. Polym. Phys. Ed.* 13, 2049 ( 1975 )
19. L. E. Alexander, 'X-ray diffraction methods in Polymer Science', Wiley Interscience, London ( 1969 )
20. A. Zwijnenburg, PhD thesis, State University of Groningen, the Netherlands ( 1978 )
21. B. Wunderlich, *Polymer* 5, 125 & 611 ( 1964 )
22. E. Hellmuth, B. Wunderlich, *J. Appl. Phys.* 36, 3039 ( 1965 )
23. A. Zwijnenburg, P. F. van Hutten, A. J. Pennings, H. D. Chanzy, *Coll. Polym. Sci.* 256, 729 ( 1978 )

Accepted October 12, 1987 C